Effect of pulsed laser irradiation on the SiC surface

Manuela Suess[1], Christian Wilhelmi[2], Milena Salvo[3], Valentina Casalegno[3],

Peter Tatarko[4], Matthias Funke[1]

[1]Airbus DS GmbH, Space Systems, Mechanical Products and Engineering GE, Friedrichshafen, Germany

[2]Airbus Defence and Space GmbH, Airbus Group Innovations, Materials Structures and Manufacturing Technologies, Munich, Germany

[3]Department of Applied Science and Technology, Politecnico di Torino, Torino, Italy

[4]Nanoforce Technology Ltd., Queen Mary University of London, London, UK

Abstract

The effect of a pulsed laser irradiation (Nd:YVO$_4$, 1064 nm) in air on the surface morphology and chemical composition of silicon carbide and on the adhesion with an epoxy adhesive was investigated. Scanning and transmission electron microscopies, atomic force microscopy, and X-ray photoelectron spectroscopy revealed that the laser treatment reduced the contamination level of the surface and induced the formation of a silica-based nanostructured columnar layer on the SiC surface. The mechanism for the formation of five different microstructural regions is described in this paper. In addition, the formation of a 5-10-nm-thick

graphite layer between the oxide layer and SiC was observed. The joining test with Hysol® EA9321 showed that the nanostructured columnar silica layer was completely infiltrated by the adhesive, thus leading to a significant increase in the joined specific area and a mechanical interlocking at the adhesive/substrate inter- face. Nevertheless, the apparent shear strength of the joined SiC samples slightly decreased after the laser processing of the surfaces from about 42 MPa for lapped SiC to about 35 MPa for laser-nanostructured SiC. The formation of the graphite layer was found to be responsible of the poor adhesion properties of the SiC sur- faces modified by the laser radiation.

KEYWORDS

adhesives/adhesion, graphite, laser, silicon carbide

1. INTRODUCTION

In the aerospace industry, there is a strong demand for the use of specific materials to face harsh operational conditions in conjunction with high performance and reliability. In the past decades, Airbus DS GmbH (former EADS Astrium) developed, in collaboration with a ceramic manufacturer (BOOSTEC Industries, France), the Sintered Silicon Carbide (S-SiC) technology for space applications, ie, large ultrastable lightweight optical instruments.[1,2] Several projects for space based on telescopes and mirrors, such as Herschel, Gaia, and NIRSpec[3-5] exploit the outstanding properties of this SiC material, among them the excellent microstructural and compositional homogeneity, the low residual internal stresses, the isotropic, and low coefficient of thermal expansion (CTE) as well as the excellent thermal and mechanical properties.[6]

Beside the material manufacturing process, several assembly techniques like bolting, brazing, bonding, etc.[1] were also developed to enhance SiC applications. Generally, before similar or dissimilar adhesive bonding, the SiC has to be accurately polished by an expensive lapping process, which significantly reduces the flexibility in the component design.

Previous studies, carried out by Airbus Group Innovations and Airbus DS GmbH, demonstrated that a laser radiation can be used as an alternative and effective new technology for surface pretreatment of metals and several ceramics before bonding.[7,8] When the laser treatment of the surface led to the formation of a nanostructured layer an increase in the bonding performance was always achieved.[7] The main advantages of the laser surface modification are:

1. Cleaning and activation of the surface due to a one-step pretreatment,
2. Increased surface area and enhanced mechanical/chemical anchoring of adhesive,
3. Complete dry & environmental friendly process (ie, no hazardous chemicals are used to modify the surface, REACH conform),

4. High reproducibility, the very accurate control of the process increases the quality,
5. Easy implementation in automatic and production machinery,
6. Time efficient and resource saving process (nearly no human influence).

The modification of SiC surfaces by laser ablation prior to bonding was recently proposed by Harris et al. and Starikov et al.[9-11] In these studies, the modified SiC surfaces showed a micro-pattern (micro-stripes or microcolumn arrays), which may negatively affect the mechanical properties of the ceramic material; indeed, a cohesive failure in the SiC adherents and not within the adhesive occurred when adhesively bonded joints were tested by apparent shear test in Ref.[9] Although the laser treatment improved the shear strength of the joined components, a lack of cohesive failure within the adhesive suggested that the maximum strength of the joints was not achieved.[9]

In this paper, the laser radiation in air was applied on SiC to obtain a homogeneous nanostructured oxide layer, which does not decrease the mechanical properties of the ceramic. A thorough study on the effect of the laser irradiation on the surface morphology, chemical composition, and adhesion properties of SiC was performed. For the first time, the cross section of the laser-affected zone was investigated using Focused Ion Beam technique, followed by detailed analysis of the cross sections using scanning and transmission electron microscopy. These detailed investigations led to the detection of a graphite layer at the oxide layer/SiC interface. This is the first report on the formation of such a graphite layer during laser irradiation of SiC in air and the mechanism for the formation of the laser- affected zone on SiC was proposed accordingly.

2. EXPERIMENTAL PROCEDURE

The silicon carbide used in this study was Boostec®SiC (former SiC100®) produced by Mersen (Bazet, France). It is a polycrystalline α-SiC (>98.5 wt% SiC, no traces of free silicon) obtained by pressure less sintering. Chemical composition and properties of Boostec®SiC are reported in.[6] As a reference for the bonding pretreatment, the lapped surfaces of SiC were used with a global flatness of below 5 μm.

The laser-based surface modification of SiC with as sintered surface quality was carried out with the laser system PowerLine E Air 25 from Rofin (Bergkirchen, Germany) in air. This original designed laser system is a nanosecond pulsed Neodymium-doped Yttrium-Orthovanadate laser (Nd:YVO$_4$) with a wavelength of 1064 nm. The laser system has an average supply power of 25 W and allows a pulse frequency from continuous wave (cw) up to 200 kHz. During this study, a wide parameter study was executed covering the entire power intensity spectrum of the laser system. The discussed parameters are representative for the achieved results.

Boostec®SiC samples (25x25x5 mm^3) with lapped and laser-treated surface qualities were bonded to similar SiC- SiC joints using Hysol® EA9321 (Henkel Corporation, Rocky Hill, CT), a two-component thixotropic paste adhesive, which was cured at room temperature for 8 days.

As sintered, lapped and laser-structured SiC as well as joined SiC-SiC specimen were characterized using scanning electron microscopy (SEM) with energy dispersive spectroscopy (EDS) detector (AURIGA FIB-SEM Instrument, Carl Zeiss Microscopy GmbH, Jena, Germany), transmission electron microscopy (TEM) (200 kV, JEOL 2010, FIB preparation of lamellas was done using FEI Quanta 3D FEG 200/600, FEI Company, Hillsboro, OR), Atomic force microscopy (AFM) (Innova, Bruker Corporation, Boston, MA, analyses performed in tapping mode), and X-ray photoelectron spectroscopy (XPS) (Quantum 2000 Scanning ESCA Microprobe, Physical Electronics GmbH, Ismaning, Germany). The SEM analysis for lateral view of some the laser-treated SiC was performed on fractured surface achieved by cutting with a diamond wire saw (Modell 6234, Mannheim, Germany) from the back side up to 0.5-1.0 mm and the sample was then broken up after cooling in liquid nitrogen.

The sessile drop technique was used to measure the sur- face wettability and energy of lapped and laser-structured SiC (Drop Shape Analyzer DSA100, Kruss GmbH, Hamburg, Germany). Distilled water and glycerol were used to determine the surface energy using the Owens and Wendt method.[12]

The mechanical properties of SiC after laser treatment was evaluated by the co-axial ring in ring test according to DIN EN1288-5[13] with a statistic of six samples.

The mechanical strength (apparent shear strength) of the joined samples was determined using a single lap offset (SLO) test in compression according to a method adapted from standard ASTM D1002-05 (universal testing machine SINTEC D/10).[14] The dimensions of the samples are reported in Figure 1. The samples were bonded with a joining area of 12.5x25 mm^2 and a bonding gap thickness of 0.3 mm. For each joint three samples were tested. All the fracture surfaces were macroscopically characterized according to DIN EN ISO 10365.15
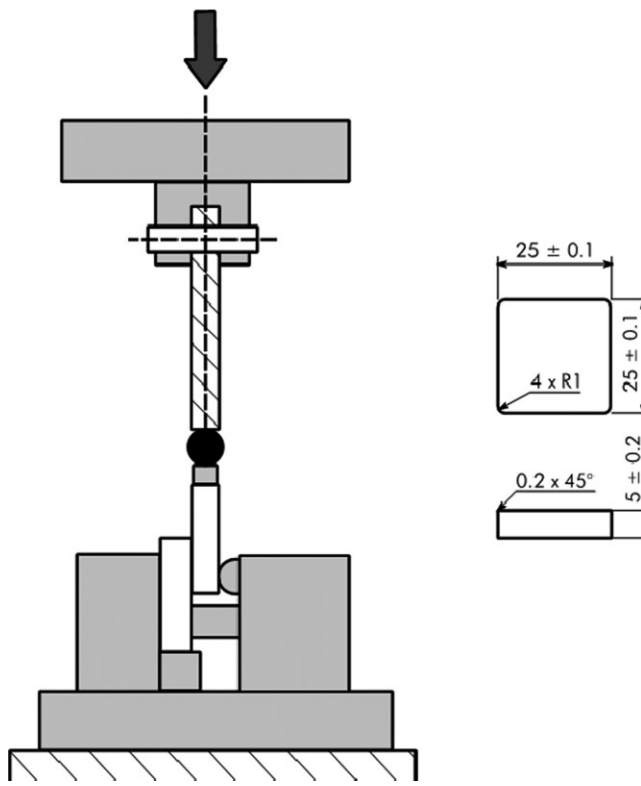
FIGURE 1 Sample and test configuration for the single lap offset test

3. RESULTS AND DISCUSSION

3.1 Surface morphology and chemical characterization

Figure 2A, B show the surface morphology of as sintered and lapped SiC, respectively. The residual porosity observable on as sintered and lapped SiC surfaces is due to the pressure less sintering process and was estimated to be about 2% in volume with a fine SiC powder grain size of <1 μm up to 2 μm (Figure 2A).[1]

Figures 2C,3 show the morphology of the SiC surface after laser treatment that led to the formation of a homogeneous open porous nanostructure. The laser-structured zone consisted of the agglomerates of spherical nanoparticles that had an average diameter of about 5-30 nm (Figure 2C). The cavities between the single agglomerates (red arrows in Figures 2C,3 and 4) define, with their size and number, the degree of open porosity formed on the surface during the laser treatment. As shown in the lateral view of the laser treated as sintered SiC in Figure 4, when the laser parameter set-up was optimized, the cavities and agglomerates were homogenously distributed in both orientations, parallel and perpendicular to the surface, and formed a nanostructured columnar thin film on the SiC surface (~1 μm thick). This peculiar morphology led to an extensive increase in the surface area that, when completely penetrated by the adhesive, should create a mechanical anchoring system expected to enhance the mechanical performance of bonded samples.

Table 1 shows the chemical composition of the as sintered and the laser-treated SiC surfaces as quantified by XPS. The position O1s peak at 532.9 eV and Si2p peak at
103.5 eV, found in spectra of the laser-treated surfaces (figures not reported here), were consistent with the Si-O bonds in SiO_2.[16] This indicates that the nanostructured columnar layer formed during laser irradiation in air is primarily composed of silica SiO_2.

Furthermore, after the laser process in air, it was found that the carbon content was reduced for all laser parameter set-ups to less than 5 at. % in comparison with the usual content on the as sintered SiC of about 25 at. % or higher (C nonbonded to Si as Si-C). From dedicated carbon C1s spectra (figures not reported here) it is assumed that this is adventitious C (carbon contamination originating from the environment). These results demonstrate that the laser treatment had a cleaning effect and led to a significant reduction in surface contamination, as already observed by Kurtovic et al.[7] on laser-treated Ti alloy. The cleaning effect on the SiC surface was found to be stable after four weeks of storage in laboratory environment, only wrapped in a laboratory wipe and aluminum foil.
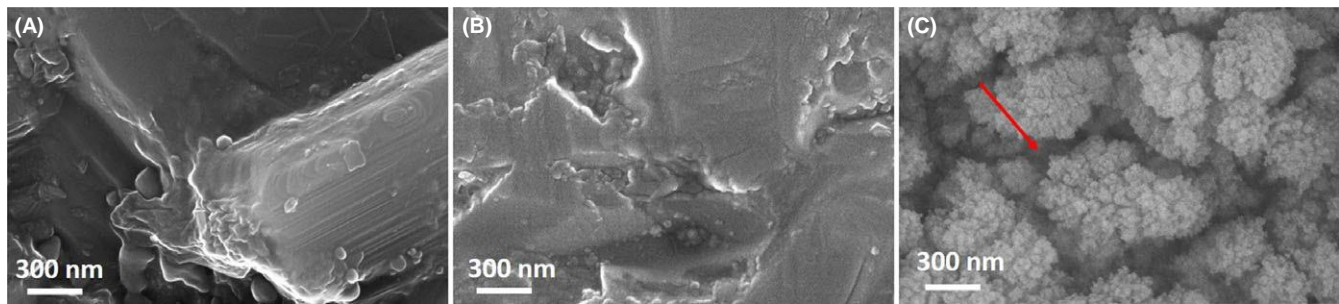
FIGURE 2 SEM micrographs showing the top view of the (A) as sintered SiC, (B) lapped SiC, and (C) laser-treated SiC.
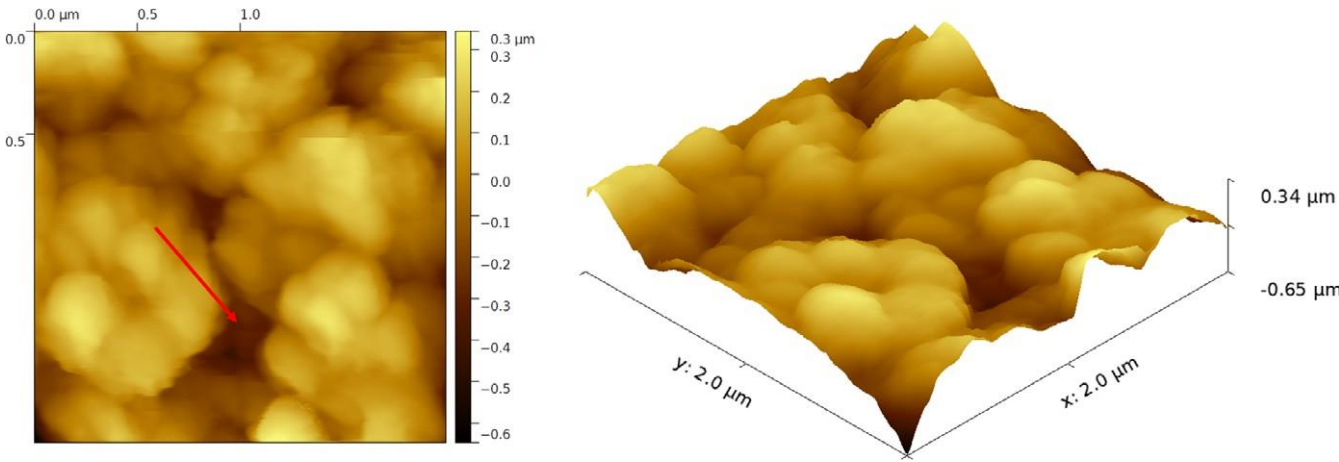

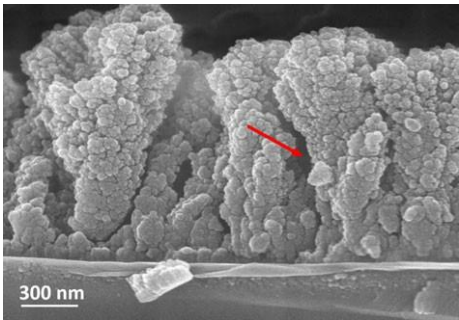FIGURE 3 Atomic force microscopy images of the laser-treated SiC surface.

FIGURE 4 SEM micrograph showing the lateral view of the laser-nanostructured SiC surface.

TABLE 1 Chemical composition of the as sintered and laser- treated SiC surfaces as quantified by XPS

Element	C	N	O	Si	Na
As sintered SiC [at.%]	44.6	14.6	18.8	21.3	0.7
Laser-treated SiC [at.%]	3.7	–	70.3	26.0	–

TABLE 2 Contact angle and surface energy for lapped SiC and laser-treated SiC

	Angle (°)		Surface energy (mJ/m²)		
Sample	Water	Glycerol	Polar	Dispersive	Total
Laser-treated SiC	15	33	79	3	82

The sessile drop technique was used to determine the effect of the nanostructured columnar silica layer formation on the wettability. The results are shown in Table 2, where the surface energy has been divided into polar and dispersive components using Owens and Wendt's method. It was found that the laser treatment significantly increased the wettability and surface energy with a very high contribution of the polar component. The measured values are in agreement with the wettability and surface energy measured by Harry et al. for laser-processed SiC and they were expected to improve the adhesive bonding

strength.[9]

3.2 Mechanical strength of bulk SiC and joints

The co-axial ring in ring test was performed, according to DIN EN1288-5, to evaluate the effect of the laser treatment on the mechanical strength of Boostec®SiC. During the test, the tensile stress is increased at a constant rate and the most severely stressed region corresponds to the lower surface area defined by the loading ring. Any surface damage would cause a significant reduction in strength of the ceramic.

The bending strength of SiC after laser treatment was 383 ± 28 MPa. This value is comparable with the reference value of 354 ±26 MPa (lapped SiC), thus demonstrating that the laser treatment had no detrimental effect on the mechanical properties of the bulk SiC material.

In addition, after the mechanical tests, the fractography was performed to study the initial crack propagation. All samples (reference and laser treated) showed that the initial crack started inside the bulk SiC material at pores originating from the SiC manufacturing process. Figure 5 exemplarily shows the cross section of the laser treated as sintered SiC material and the large size ratio between a manufacturing process-related pore and the laser-induced surface morphology.

The single lap offset (SLO) test in compression was used to evaluate the adhesion properties of SiC surfaces after laser treatment from low to high-energy densities. The selected adhesive, Hysol® EA9321, is thixotropic two c o m p o n e n t s epoxy paste glue, which is well-known in the space industry. This adhesive is characterized by a good toughness as well as stable strength values up to about 80°C.[17]
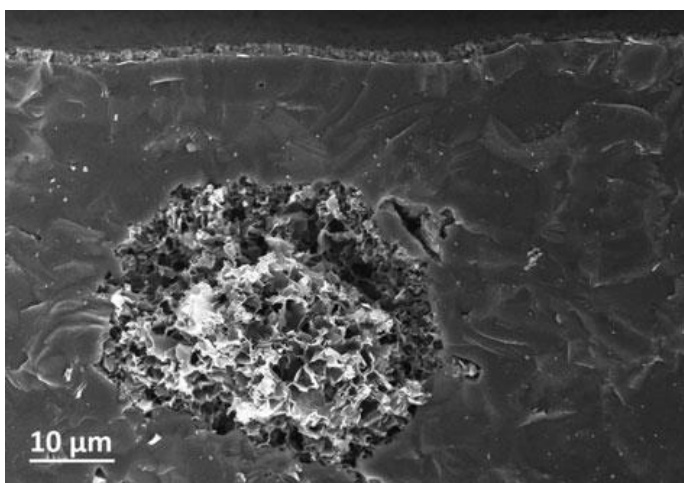

FIGURE 5 SEM cross section of laser-treated SiC with the nanostructured silica layer on the top covering the SiC surface and a large pore in the ceramic formed during the manufacturing process of the SiC

The measured apparent shear strength of the lapped SiC-SiC joints showed a reference value of 41.6 ±0.9 MPa and could not be reached by the laser- treated joined SiC samples, with a value of 34.8 ± 3.4 MPa. This apparent shear strength of about 35 MPa is a satisfactory value and, for a lot of applications, it would meet the mechanical requirements. However, it was the first time that the nanostructured modified surface obtained with the laser irradiation before bonding resulted in complete adhesive failure behavior. According to previous studies, carried out at Airbus Group Innovations and Airbus DS GmbH, on laser nanostructuring of different metallic and ceramic material surfaces, a cohesive failure mode in the adhesive was expected for the joints with laser pretreated bonding partners.[7] However, the fracture surface characterization (Figure 6) evidenced adhesive failure mode for all investigated samples (lapped and laser-treated SiC-SiC joints). Furthermore, the adhesively failed surface showed a very intense shiny surface characteristic, much more than the lapped SiC surface (Figure 6). This is a further indication for an unexpected failure mode occurred in combination with the laser irradiation of SiC, which differs from all previous investigated and assessed materials.

3.3 Characterization of the laser-affected zone

For a better understanding of the failure mechanism, further analyses were carried out to investigate the morphology and the composition of the laser-affected SiC.

Figure 7 shows FIB lamella preparation of a laser treated SiC/Hysol® EA9321/laser-treated SiC joint and a higher magnification at the interface between the silica-nanostructured columnar structure and the adhesive. The adhesive completely infiltrated the columnar layer and air inclusions or unfulfilled cavities were not observed in this area. This was exemplary for all the investigated materials and confirmed that the infiltration of the adhesive was always about 100%. As

discussed above, the penetration of the adhesive in the nanostructured layer should create a mechanical anchoring system expected to enhance the mechanical strength of bonded samples and cohesive failure. Despite excellent infiltration of the adhesive was observed, the improvement of the mechanical behavior was not achieved for these laser-treated SiC samples. Figure 7 (highest magnification micrograph) shows that, during the FIB lamella preparation, a crack propagated along the nanostructured columnar SiO_2 layer/SiC interface, thus revealing the formation of a weakly bonded interface in the laser-treated SiC. SEM analyses on the fracture sur- faces after mechanical tests confirmed that the adhesive failure occurred at the SiO_2/SiC interface in all the samples.

The cross section of a typical laser-affected SiC surface is shown in Figure 8, where different regions can be identified as indicated by the red arrows; from the bottom to the top: (i) the SiC unaffected by the laser irradiation; (ii) a biphasic region with a round shaped phase (black in the picture) surrounded by a second phase (gray color); (iii) a few nm thick single phase region; (iv) a dense silica layer, and (v) the nanostructured columnar silica layer. To investigate with more details, the composition of the different regions, TEM analysis was performed at the SiO_2/SiC interface.
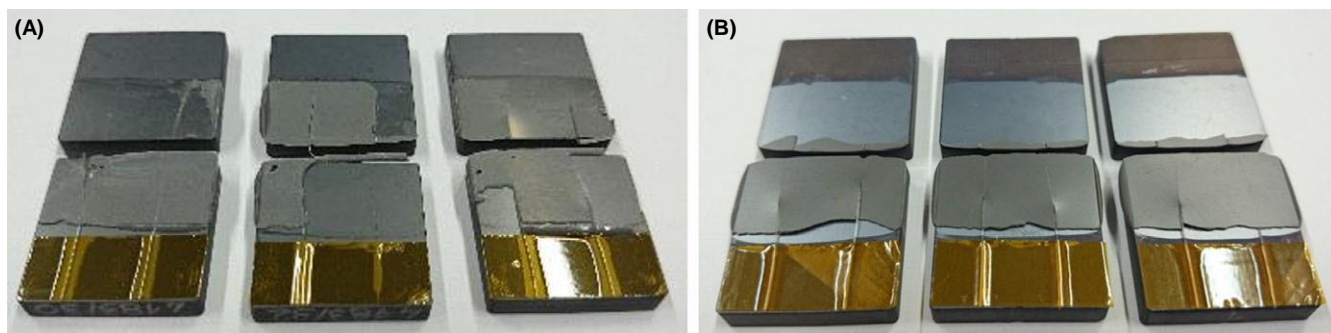

FIGURE 6 Fracture surfaces of (A) lapped SiC/Hysol® EA9321/lapped SiC and (B) laser-treated SiC/Hysol® EA9321/laser-treated SiC joints after single lap offset test.
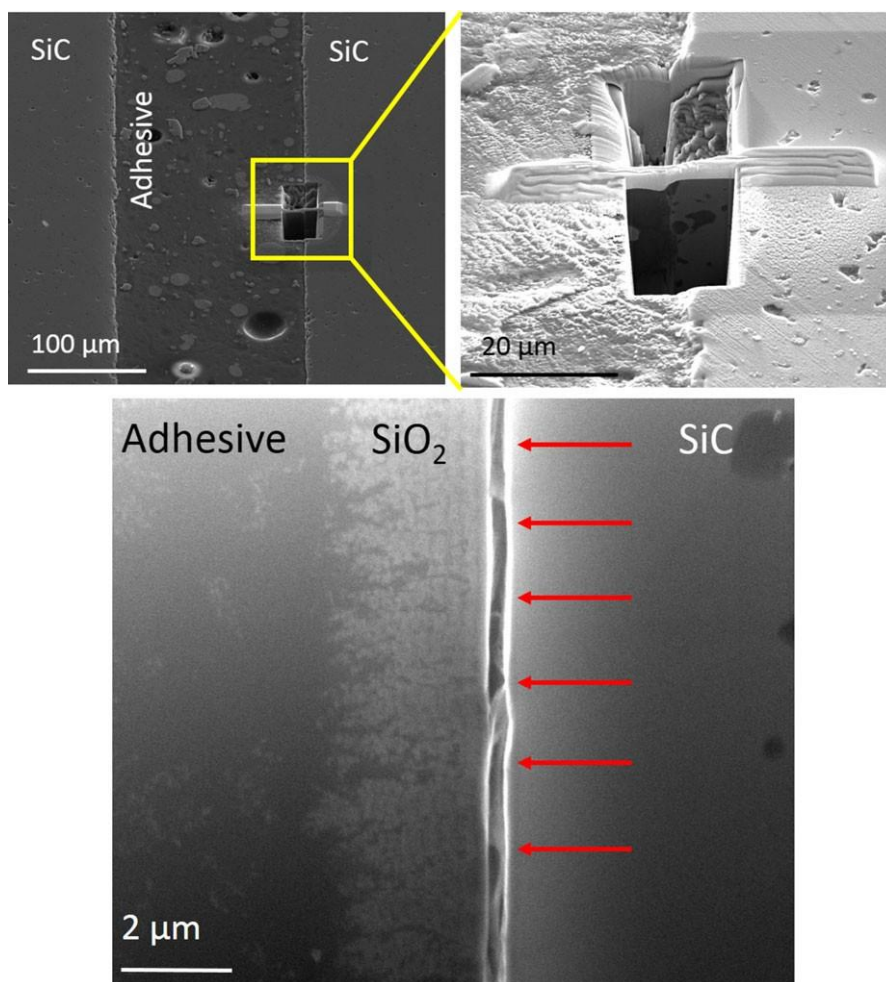

FIGURE 7 FIB lamella preparation of SiC-SiC joints, laser structured, bonded with adhesive Hysol® EA9321, after failure at the

In Figure 9A (TEM image) the SiC bulk, unaffected by the laser treatment, corresponds to the large grains (about 2 μm size) visible on the top right side; between the large SiC grains and the silica layer a nanostructured area was clearly observed (its thickness was from ~100 to 250 nm). At a higher magnification (Figure 9B), it is evident that the biphasic region (identified in Figure 8) was formed by nanosize SiC and onion rings-like graphite. The carbon onions had a size in the range 10-30 nm (Figure 10). The formation of a C-rich layer during the laser treatment in air was also confirmed by XPS depth analysis. The carbon C1s spectra showed a shoulder around 284 eV consistent with C-C bond. Moreover, Gorelik et al.[18] observed the formation of onion-like carbon clusters embedded in crystalline SiC after laser-induced crystallization of amorphous SiC.

In addition, Figures 9,10 show that a homogeneous graphite layer was formed between the nanosize SiC and the silica. The graphite layer was present along the entire sur- face and had a thickness ranging between 5 and 10 nm. Because of its lamellar structure, the graphite layer was responsible for the poor adhesion properties of the laser treated as sintered SiC. It acted as a lubricant material at the interface and caused the adhesive failure behavior. The XPS analyses on the fracture surfaces after the mechanical tests revealed a very high concentration of C (~90%) on both surfaces, suggesting that the crack initiated and propagated within the graphite layer.

The formation of C-rich regions in SiC during Nd:YAG lasers irradiation has been widely discussed in literature,[19-21] but, to the best of the authors' knowledge, a coherent and continuous graphite layer covering the SiC surface has never been observed in SiC materials after laser irradiation neither in vacuum, inert gas nor air conditions.
C-rich layers at the SiO_2/SiC interface were observed after thermal oxidation processes of semiconductor SiC involving long dwelling time (several hours).[22] Katsui et al.[23] discussed the formation of a 40-nm-thick carbon layer between SiC and SiO_2 scale during the passive oxidation of SiC at 1600°C for 40 hours. The reaction kinetics and the mechanisms leading to the formation of the C-rich layer, discussed in these previous studies, cannot be applied to the phenomenon observed in this work since the duration of the laser treatment in air was only few nanoseconds, between 10 and 50 ns.
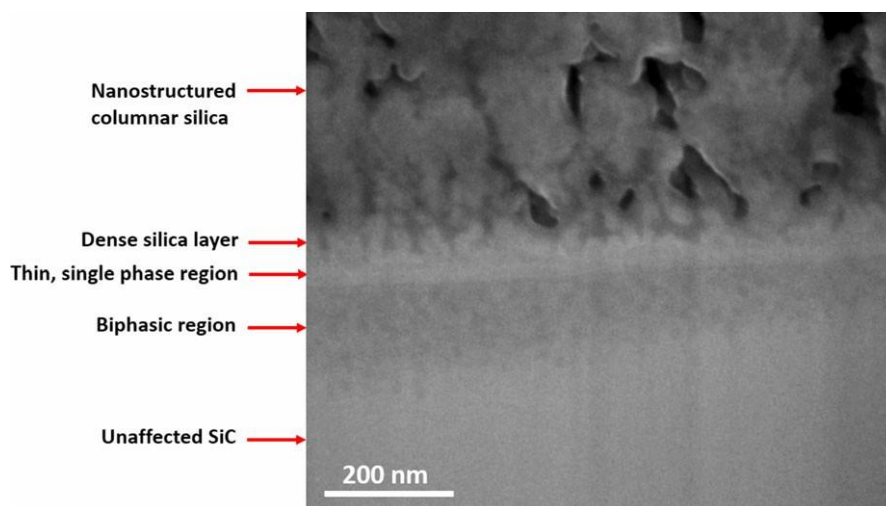

FIGURE 8 SEM micrograph showing the cross section of the laser-affected zone in SiC.
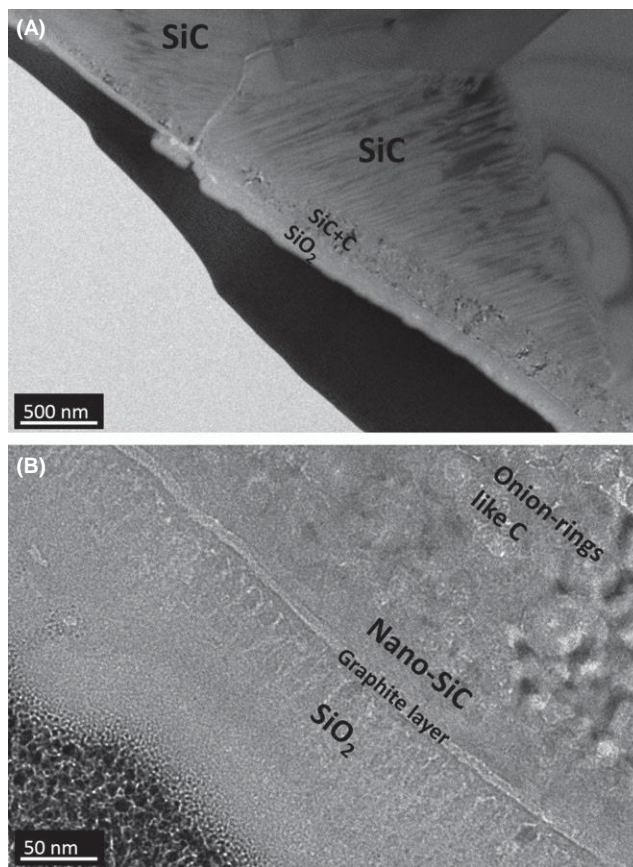
FIGURE 9 TEM images showing the cross section of a laser- treated SiC: (A) affected and unaffected zones; (B) a higher magnification of the laser-affected zone
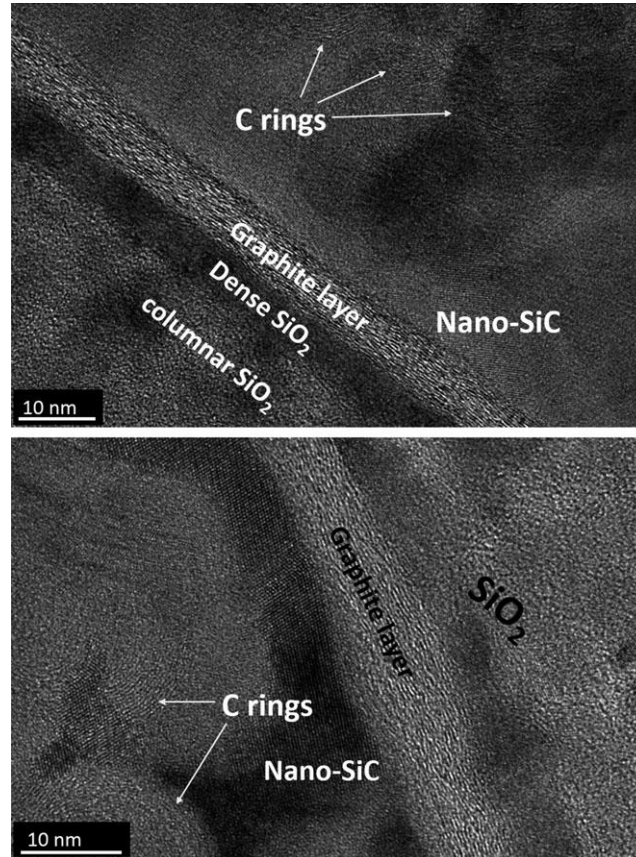

FIGURE 10 TEM images showing the cross section of a laser- treated SiC in the laser-affected zone

According to the TEM and SEM analysis, the microstructure of the laser affected zone of SiC can be summarized as in Figure 11. The following mechanism for the formation of the different regions is proposed:
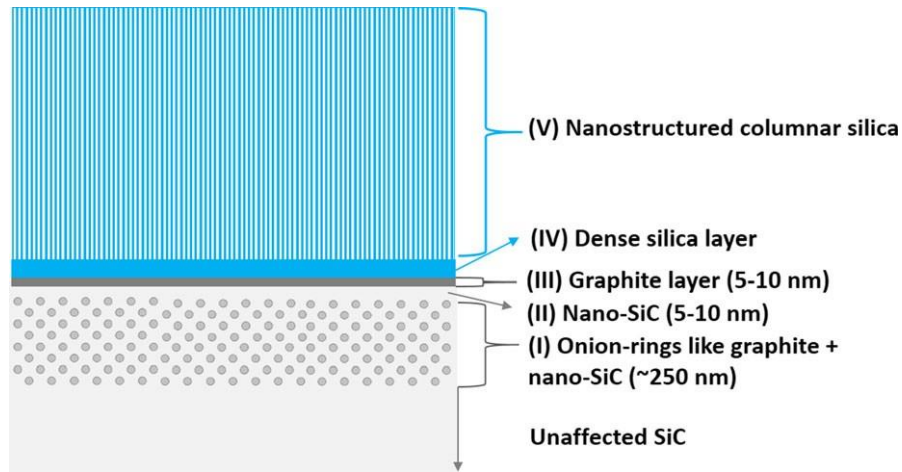

FIGURE 11 Schematic of the microstructure of the laser-affected zone of SiC: five different regions were identified.

1. During the laser pulse (10-50 ns) in air, the laser affected zone (~200-300 nm) reached very high temperatures, well above the melting temperature of SiC. At about 2830°C, Figure 12,[24] incongruent melting of SiC leads to the formation of a Si-rich liquid and C .

Vaporization of both Si as gaseous SiO and/or Si (boiling point at ~3250°C), and C as CO, can occur at the sur- face in contact with air. In the region beneath the surface, the formation of volatile oxides was limited by the diffusion of oxygen through the liquid, while the vaporization of Si caused a deviation from the 1:1 stoichiometry of the SiC system, increasing the C content in the liquid phase (region I in Figure 11). Because of the gradient of C con- centration and its high affinity with oxygen, C in excess near the surface could quickly diffuse into the liquid to the interface with air, forming a thin graphite layer (region III in Figure 11) on an almost stoichiometric 1:1 Si:C region (region II in Figure 11).

2. As soon as the laser pulse stopped, the sample was subjected to an ultrafast cooling that determined the formation of the complex nanostructure. At temperatures below the peritectic temperature, the C-rich region solidified in a mixture of two solid phases, SiC+C, as foreseen by the SiC phase diagram in Figure 12. This biphasic region was characterized by onion rings like C embedded in nano-SiC (region I in Figure 11).

In addition, a liquid silica layer, deriving from the reaction between SiO and O_2 condensed on the graphite layer (layer IV in Figure 11). The silica layer limited the diffusion of O_2 to the SiO_2/C interface and of CO outward, thus inhibiting the oxidation of the graphite layer, which was observed to be stable in the laser process conditions used in this study.

At temperatures below the melting point of SiO_2 (~1720°C), the nucleation and growth of nanostructured and granular columnar silica occurred via a vapor-solid mechanism (region V in Figure 11).[25,26]
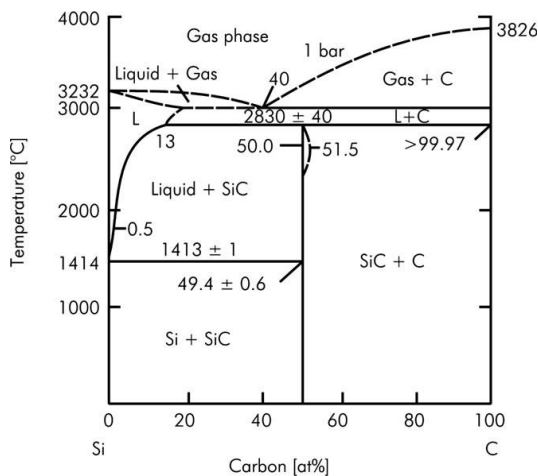

FIGURE 12 Si-C phase diagram from[24]

4 CONCLUSIONS

The effect of the laser irradiation (Nd:YVO$_4$, 1064 nm) in air on the surface morphology, chemical composition, and the adhesion properties with the adhesive Hysol® EA9321 was investigated. X-ray photoelectron spectroscopy showed that the laser treatment had a cleaning effect and led to a
significant reduction in surface contamination. Moreover, the cleaning effect on the SiC surface was found to be stable after four week storage in laboratory environment. In previous studies at Airbus Group, the laser induced sur- face nanostructuring of several metals and ceramics was successfully used as pretreatment for adhesive bonding leading to higher mechanical properties of joints and cohesive failure in the adhesive. The effectiveness of the laser treatment can be attributed to the formation of a nanostructured columnar thin film on the substrates to be joined, which creates a mechanical anchoring system when penetrated by the adhesive. After the laser irradiation in air, the formation of a homogeneous and nanostructured columnar silica layer on SiC surface was observed and the adhesive, Hysol® EA9321, completely infiltrated the open porosity of the layer. Nevertheless, the mechanical strength of adhesively bonded laser-treated SiC was lower than the reference one (lapped SiC) and the failure mode was always adhesive. For the first time, a thorough investigation of the cross section of the laser-affected zone using Focused Ion Beam technique, followed by detailed analysis using SEM and TEM, showed that a stable 5-10-nm-thick graphite layer was formed at the SiO$_2$/SiC interface and was responsible for the poor adhesion properties of the laser-nanostructured SiC. The mechanism for the formation of the different microstructural regions identified after laser-pulsed irradiation of the SiC surface is proposed based on the obtained results.

REFERENCES

1. Breysse J, Castel D, Laviron B, Logut D, Bougoin M. All-SiC Telescope Technology: Recent Progress and Achievements. In: *Proceedings of the 5th International Conference on Space Optics (ICSO 2004)*, Toulouse, France, 30 March–2 April, 2004.

2. Spanò P, Zerbi FM, Norrie CJ, et al. Challenges in optics for extremely large telescope instrumentation. *Astron Nachr*. 2006;88:789–811.

3. Toulemont Y, Doyle D, Pierot D, Rivière R. Development and Per- formance of a 3.5 m all SiC Telescope for HERSCHEL. In: *Pro- ceeding of OPTRO 2010, International Symposium on Optronics in Defence and Security, Space*. Paris, France, 3–5 February, 2010.

4. Charvet P, Pierot D, Fruit M, Coatantiec C, Garè P. The GAIA Astrometry Mission: Status of Optical Development. *Proceeding of OPTRO 2010, International Symposium on Optronics in Defence and Security, Space*. Paris, France, 3–5 February, 2010.

5. Honnen K, Kommer A, Messerschmidt B, Wiehe T. NIRSPpec OA Development Process of SiC Components. *Proceeding of the SPIE, Advanced Optical and Mechanical Technologies in Telescopes and Instrumentation*. Marseille, France, June 23, 2008.

6. Boostec®SiC data sheet. Available at https://www.mersen.com/f ileadmin/user_upload/pdf/ht/21-silicon-carbide-sic-boostec-mersen. pdf. Accessed May 15, 2016.

7. Kurtovic A, Brandl E, Mertens T, Maier HJ. Laser induced sur- face nanostructuring of Ti-6Al-4V for adhesive bonding. *Int J Adhes*. 2013;45:112–117.

8. Brandl E, Kurtovic A, Wilhelmi C. Method for the Nanostructur- ing of Ceramic, Glass, Carbon, Boron, Silicon and Compound Materials. EU Patent application EP20130002753, 2013.

9. Harris AJ, Vaughan B, Yeomans JA, Smith PA, Burnage ST. Surface preparation of silicon carbide for improved adhesive bond strength in armour applications. *J Eur Ceram Soc*. 2013;33:2925– 2934.

10. Starikov D, Pillai R, Glenn T, et al. Improvements in bonding of silicon carbide ceramic to metals. *Int J Mater Eng*. 2014;4:196– 202.

11. Starikov D, Bensaoula A. Method of Bonding Solid Materials. U.S. Patent US 8,962,151 B2, 2015.

12. Owens DK, Wendt RC. Estimation of the surface free energy of polymers. *J Appl Polym Sci*. 1969;13:1741–1747.

13. DIN EN 1288-5 (2000-09) standard. Glass in Building – Deter- mination of the Bending Strength of Glass – Part 5: Coaxial Dou- ble Ring Test on Flat Specimens with Small Test Surface Areas.

14. ASTM D1002-05. Standard Test Method for Apparent Shear Strength of Single-Lap-Joint Adhesively Bonded Metal Speci- mens by Tension Loading (Metal-to-Metal), 2005.

15. ISO 10365 standard. Adhesives – Designation of Main Failure Patterns, 1992.

16. Hijikata Y, Yaguchi H, Yoshikawa M, Yoshida S. Composition analysis of SiO$_2$/SiC interfaces by electron spectroscopic mea- surements using slope-shaped oxide films. *Appl Surf Sci*. 2001;184:161–166.

17. Henkel Hysol® EA9321 data sheet. Available at: http://www.na.henkel-adhesives.com. Accessed May 15, 2016.

18. Gorelik T, Urban S, Falk F, Kaiser U, Glatzel U. Carbon onions produced by laser irradiation of amorphous silicon carbide. *Chem Phys Lett*.

2003;373:642–645.

19. Pecholt B, Gupta S, Molian P. Review of laser microscale pro- cessing of silicon carbide. *J Laser Appl*. 2011;23:012008.

20. Salama IA, Quick NR, Kar A. Microstructural and electrical resistance analysis of laser-processed SiC substrates for wide bandgap semiconductor materials. *J Mater Sci*. 2005;40:3969– 3980.

21. Pehrsson PE, Kaplan R. Excimer laser cleaning, annealing, and ablation of b-SiC. *J Mater Res*. 1989;4:1480–1490.

22. Chang KC, Nuhfer NT, Porter LM, Wahab Q. High-carbon con- centrations at the silicon dioxide–silicon carbide interface identi- fied by electron energy loss spectroscopy. *Appl Phys Lett*. 2000;77:2186.

23. Katsui H, Oguma M, Goto T. Carbon interlayer between CVD SiC and SiO_2 in high-temperature passive oxidation. *J Am Ceram Soc*. 2014;97:1633–1637.

24. Kleykamp H, Schumacher G. The constitution of the silicon-car- bon system. *Ber Bunsenges Phys Chem*. 1993;97:799–804.

25. Zhang Y, Liu Y, Liu M. Nanostructured columnar tin oxide thin film electrode for lithium ion batteries. *Chem Mater*. 2006;18:4643–4646.

26. Casalegno V, Rizzo S, Canavese G, Ventrella A, Salvo M, Ferraris M. Synthesis and characterization of SiO_2 nano- and microwires by a non-catalytic technique. *J Mater Sci*. 2013;48:6108-6114.